An Optimized Distributed Routing Protocol for Energy Management Systems Based on Wireless Sensor Networks in Intelligent and Smart Structures

Original Scientific Paper

Ahmed Hammad
University of Mansoura,
Faculty of Engineering, Department of Electronics and Communications Engineering
Mansoura, Egypt
Khairtahmed@yahoo.com

M.A. Mohamed
University of Mansoura,
Faculty of Engineering, Department of Electronics and Communications Engineering
Mansoura, Egypt
mazim12@mans.edu.eg

Heba M. Abdel-Atty
University of Port Said,
Faculty of Engineering, Department of Electrical Engineering
Port Said, Egypt
Heba.Mohamed@eng.psu.edu.eg

Abstract – *Energy and spectrum efficiency for energy management systems based on wireless sensor networks in intelligent structures and powered by ambient energy harvesting (EH) are the main problems in wireless sensor networks. Herein, we consider relay selection methods. To address this issue, we proposed the optimal multiantenna power beacon opportunistic relay selection (OMPB-ORS) protocol, which uses decoding and forward methods, in which the relay wireless sensor nodes and the second source are energy-restricted and can harvest energy from a power beacon (PB) multiantenna to transmit aggregated information data from source to destination. The proposed protocol based on specific switching time receiver architecture enhances end-to-end performance for maximum hardware impairments and interference for the transceiver. To evaluate the performance, we compared our proposed protocol with best ORS (B-ORS), conventional ORS (C-ORS), and hybrid partial relay selection (H-PRS) protocols. Using the Rayleigh-fading channel, the simulation is driven based on asymptotic and exact form expressions of throughput (TP) and outage probability (OP). Simulation results show that the OMPB-ORS protocol achieves a higher TP and OP than all compared protocols.*

Keywords: *wireless sensor networks, energy harvesting, multiantenna power beacon, partial relay selection, opportunistic relay selection, hardware malfunctions.*

1. INTRODUCTION

Wireless sensor networks, which provide their energy from ambient energy harvesting (EH), have recently been listed as a promising technique to fix the famous problem of energy constraint for energy management systems in intelligent structures [1]. The communication equipment is outfitted with circuits that can harvest energy from the surrounding natural environment [1, 2]. In [3], the authors designed simultaneous wireless information and power transfer (SWIPT) systems. However, SWIPT systems are suited only for short-distance transmission because of a large operational sensitivity gap between the decoder and the energy harvester. In [4], the authors designed a novel system to deal with this issue in which power beacons (PBs) are used to activate wireless equipment. In [5, 6], to achieve maximum energy transfer and data rate for multiple input and output (MIMO) systems, the authors built a SWIPT receiver for the broadcasting system.

Recently, various PB-assisted wireless sensor networks using EH have been studied [7]. In [8], the authors proposed a novel hybrid wireless network with PBs deployed randomly in the area to offer mobiles an almost limitless battery life. In [7], using TDMA, the authors analyzed multiple-user wireless throughput (TP) for distributing Nakagami-m fading. Device-to-device (D2D) systems also deliberate PB-assisted techniques [9] because of the advantages of D2D systems, such as high spectral efficiency, low latency, and low-power transmission [10].

In contrast, besides the energy problem, the issue of spectrum scarcity needs a solution. In [11], the authors introduced the concept of cognitive radio (CR), where licensed primary users (PUs) can share their bands with unlicensed secondary users (SUs), provided the primary network's quality of service (QoS) is maintained. Generally, secondary users must know if PUs are available or not to use empty bands or shift to another spectrum [12, 13]. For CR WSNs, several spectrum-sensing models were created and compared [14, 15]. The benefits of CR WSNs and the significant differences between the three types of wireless sensor networks: CR WSNs, conventional WSNs, and ad hoc CR networks were also discussed in [16, 17]. Recently, various CR protocols were proposed and developed to ensure that SUs continue their operation [18, 19]. SUs are permitted to use the licensed bands simultaneously as PUs if the secondary transmitters adjust their broadcast power to meet a PU-imposed interference constraint. In [20,21], the authors improved the performance of the secondary network with vital technology, called cooperative relaying algorithms, due to the capacity to increase the performance gains. In [22], two relaying methods, such as partial relay selection (PRS) and opportunistic relay selection (ORS), have been extensively inspected. In PRS, the relay selection depends on the channel state information (CSI) for the source relay network. In ORS, the perfect relay must be selected to maximize the signal-to-noise ratio (SNR) end-to-end (e2e) between the transmitter and the receiver. In [23], the authors evaluated the performance of dual-hop CR WSNs in the existence of hardware noises and proposed three relaying algorithms, namely, best ORS (B-ORS), conventional ORS (C-ORS), and hybrid PRS (H-PRS) protocols. However, researchers proposed a better PRS scheme, where CSIs of the relay-destination connections are used to choose the relay [24]. In [23–29], several relay selection methods have been described in CR networks. Especially in [23], the PRS and ORS methods evaluated the overall performance in terms of bit error rate (BER) and outage probability (OP).

CR and EH were used in wireless sensor networks to solve the two main problems concerning energy and spectrum efficiency. In [30], the authors make SUs pick a channel to enter the harvested energy or data transmission. In [31], the authors use several SUs and various channels to fix the RF energy harvesting optimization problem for CR wireless networks. Specifically, a system model proposed by the authors where PUs take channels and make them busy, creating a chance for SUs to harvest energy and conserve it in the battery, then use the saved energy in the transmission process via an empty channel. In [32], the authors give a detailed analysis of the performance of a two-way CR EH-TWCR wireless network (EH-TWCR), which is based on decode-and-forward (DF) in the existence of transceiver limitations. In [19,20,24,25,33,34], the authors proposed the performance of multihop CR wireless networks, specifically end-to-end, where PB or RF signals of the primary transmitter can be used from SUs to harvest energy.

Because of the low-cost transceiver equipment, wireless sensor nodes fall victim to hardware limitations due to amplifier nonlinearities and phase noise [24, 26, 35, 36, 43]. The performance degradation can be recovered using a cooperative relaying algorithm. In [35], the effect of hardware failures on Nakagami-m fading channels in dual-hop relaying networks was investigated. In [36], in underlay CR networks, the performance of two-way relaying systems with hardware faults using EH relays were examined.

The contributions made by this work are as follows:

- A multiantenna PB wireless-powered cooperative communication network model is proposed, in which relays and sources are not connected with a fixed power network. Instead, PBs with multiantennas are used by relays and sources to harvest energy and then aggregated data to the destination.
- The proposed model is compared with three well-known relay selection models, namely, B-ORS, C-ORS, and H-PRS models, under interference and hardware limitations. The results compare the proposed optimal multiantenna power beacon ORS (OMPB-ORS) model performance with H-PRS, C-ORS, and B-ORS protocols in terms of system EH, TP, and OP.
- Numerical simulation is used to validate and drive outage the probability and average system TP for H-PRS, C-ORS, B-ORS, and proposed model closed-form expressions.
- The effects of multiantenna PB and other system characteristics, including harvesting time, number of relays, and position on system performance, are also examined.

The remainder of the paper is laid out as follows. The system model is described in section II. Next, Section III presents the conventional relay selection techniques. Furthermore, Section IV presents the equations of system performance for OMPB-ORS, H-PRS, C-ORS, and B-ORS schemes for OP and TP. Also, Section V displays the numerical result and compares the proposed models with all mentioned models. Finally, Section VI concludes the study.

2. SYSTEM MODEL

2.1 SYSTEM DESCRIPTION

Fig. 1. shows the proposed OMPB-ORS system model. It comprises the primary and secondary networks. The dual-hop technique communicates between a source S and a destination D in the primary network. P_n refers to the main licensed users, while n ∈ (1, 2,… , N). The secondary network comprises M relays, where N > 1 is denoted by Rm, while m ∈ (1, 2,… , M). Since the source has no direct connection with the destination, the system must select a suitable relay to transfer data from the source to the destination. Because they are considered to lack an integrated power supply, both and the set of M relay nodes must harvest energy from the multiantenna PB signal to allow information transmission. The source and relays have only one antenna. Additionally, they harvest energy from PBs. Two orthogonal time slots are used to transmit data via the chosen Relay.

It is assumed that Rayleigh fading affects all channels, and that the channel gains have exponential distributions. γSR_m and γDR_m are denoted as the channel gains for S ⟶ R_m and R_m ⟶ D links, respectively. $\gamma B_k R_m$ and $\gamma B_k S$ are denoted as channel gains between PB's k-th antenna and the S and relay R_m, respectively, where k = 1, 2, …, K denotes γSP_n and $\gamma R_m P_n$ as channel gains between S ⟶ P_n and R_m ⟶ P_n links. λ_{XY} is denoted as a random variable parameter, which equals $\lambda_{XY} = 1/E\{\gamma_{XY}\}$, where (X,Y) ∈ {S, R_m, B_k, P_n, D} and the anticipated value of the random variable Z is E{Z}.

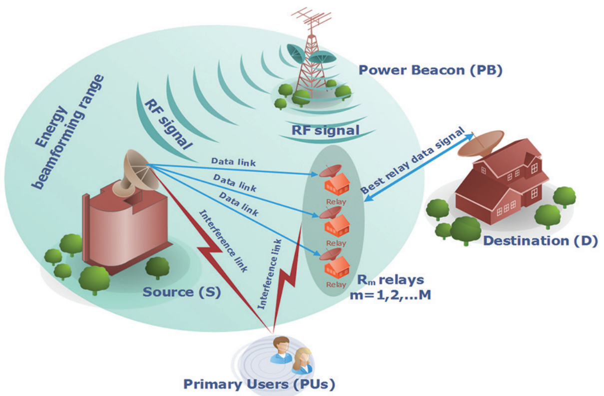

Fig. 1. System model of PB-assisted relaying protocols with relay selection methods.

The system model of the proposed protocol is implemented using the TS-HTC algorithm [37]. Fig. 2. shows that the protocol comprises three phases over the time block T, and only one node communicates at a time.

However, assuming optimal synchronization and channel state information in the network, it is beyond the scope herein to discuss how to achieve this synchronization. The batteries of S and R_m begin charging in the first phase, in which PB beamform RF signal to allow them to charge. Using the energy harvested in the first phase, S sends information to Rm. In the third phase, the best relay among the R_m relays is selected to transmit the received information from S to D by the proposed OMPB-ORS relay selection scheme or the well-known traditional relay selection schemes, i.e., H-PRS, C-ORS, or B-ORS as described in section 3.

The following set of assumptions is considered herein and in other related publications:

- A location-based clustering approach was used, in which the relays are clustered together close. This proposal is widely utilized in relay selection systems [38–40].
- As proposed in [41, 42], the PB is considered a network's devoted power source. The PB, S, R_m, and D nodes run in accordance with the harvesting energy and cooperating protocol.
- In the transmission phases, it is assumed that both the source and relay candidates exhaust their harvested energy.

2.2. HARDWARE MALFUNCTIONS

Assuming the transmitter (X) is connected with the receiver (Y), the signal-to-noise ratio of the X–Y connection can be obtained by (see [43]).

$$SNR_{XY} = \frac{P_X \gamma_{XY}}{(\tau_X^2 + \tau_Y^2) P_X \gamma_{XY} + N_0} = \frac{P_X \gamma_{XY}}{\tau_{XY}^2 P_X \gamma_{XY} + N_0} \quad (1)$$

where τ_X^2 and τ_Y^2 implement hardware malfunction levels at the transmitter and receiver, respectively, τ_{XY}^2 is the total hardware malfunctions level in the connection between transmitter and receiver, and N_0 is Gaussian noise variance at the receiver.

In the presence of Hardware malfunctions, the received signal of the X–Y link can be estimated as

$$y_{XY} = \sqrt{P_X} h_{XY} (s + \eta_{XY}) + \mu_{XY} + \upsilon_{XY} \quad (2)$$

where P_x is the power of transmitter X, h_{XY} is channel gain for X–Y link, μ_{XY} and η_{XY} are noises caused by hardware malfunctions in the receiver and transmitter, respectively, and ν_{XY} denotes the additive white Gaussian noises represented as Gaussian random variables with zero mean and variance N_0.

2.3. SIGNAL MODELING

2.3.1 EH phase

Here, the S and M relays charge their batteries by the beamform RF signal from PB, and the harvested energy by S and M relays can be formed, respectively, as

$$Q_s = \eta \alpha T P_B \sum_{k=1}^{K} \gamma B_k S \quad (3)$$

$$Q_{R_m} = \eta \alpha T P_B \sum_{k=1}^{K} \gamma B_k R_m \quad (4)$$

where PB represents the power of the transmitted signal from B, η is the efficiency of the harvested energy at S and M relays, and αT is the EH process time.

Fig. 2. shows that in the remaining (1 – α)T duration, the selected relay collaborates the source by decode and forwards the received signal. Finally, the optimal relay is chosen to transmit the S information to D once a relay selection procedure occurs. Consequently, the transmitted power at S and the set of R_m relays are expressed, respectively, as

$$E_s = \frac{Q_s}{2(1-\tau)/3} \tag{5}$$

$$E_{R_m} = \frac{Q_{R_m}}{(1-\tau)/3} \tag{6}$$

From [43] in the underlay CR with respect to interference constraint, the signal-to-noise ratio can be obtained at the 1st and 2nd hops across the relay provided by

$$SNR_{1m} = P_0 \gamma SR_m \big/ \tau_D^2 P_0 \gamma SR_m + N_0 \tag{7}$$

$$SNR_{2m} = P_m \gamma R_m D \big/ \tau_D^2 P_m \gamma R_m D + N_0 \tag{8}$$

where N_0 is the variance of the additive white Gaussian noise AWGN and

$$\Delta = P_B / N_0 \tag{9}$$

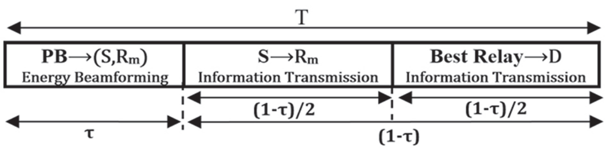

Fig. 2. Diagram of time-switching harvest then cooperate protocol (TS-HTC).

3. RELAY SELECTION SCHEMES

3.1 OPPORTUNISTIC RELAY SELECTION (ORS) SCHEME

Both channel hops are significant in the ORS relay selection method and should be considered [39, 41, and 42]. The optimal relay, which precisely maximizes the minimum number of channel strengths between S ⟶ R_m and R_m ⟶ D is selected and is provided by

$$R_S^{ORS} = \arg\max_{m \in M} \{\min(\gamma SR_m, \gamma R_m D)\} \tag{10}$$

3.2 PARTIAL RELAY SELECTION (PRS) SCHEME

This approach assumed that CSI is only valid for one hop [23, 39, and 44]. Precisely, when the CSI is available for the initial hop S ⟶ R_m, the PRS technique is denoted by PRSI. If the CSI is only accessible for the second chance R_m ⟶ D, it is termed PRSII. In PRSI and PRSII, the chosen relay can be represented as

$$R_S^{PRSI} = \arg\max_{m \in M} \{(\gamma SR_m)\} \tag{11}$$

$$R_S^{PRSII} = \arg\max_{m \in M} \{(\gamma SD)\} \tag{12}$$

3.3 PROPOSED OPTIMAL MULTIANTENNA POWER BEACON OPPORTUNISTIC RELAY SELECTION (OMPB-ORS) SCHEME

$$R_v : \min(SNR_{1v}, SNR_{2v}) = \max_{m=1,2,\ldots,M} (\min(SNR_{1m}, SNR_{2m})) \tag{13}$$

The optimal relay is chosen in the OMPB-ORS protocol to optimize the end-to-end SNR, i.e.,., where ν ∈ {1, 2,… , M}. The end-to-end performances of this scheme are then calculated as follows:

$$OP_{OMPB} = Pr(\, C_{th} > (1-\alpha)T \, log_2(\, 1 + min(\, SNR_{1v}, SNR_{2v}))) \tag{14}$$

where the C_{th} in the secondary network is the desired data rate. The end-to-end channel capacity with decoding and forward technique of S ⟶ R_m ⟶ D path is described by

$$C_{SD} = (1-\alpha)T \, log_2(\, 1 + min(\, SNR_{1m}, SNR_{2m})) \tag{15}$$

4. PERFORMANCE EVALUATION

4.1 OUTAGE PERFORMANCE OF PROPOSED SCHEME AND THROUGHPUT

The Flowchart of (OMPB-ORS) protocol scheme is shown in Fig. 3.The TS-HTC algorithm [37] was used in the proposed protocol, and the other three protocols used the TSR Protocol [23]. This approach made the difference in results clear, in favor of our protocol. The end-to-end OP can be defined as the probability that a positive threshold C_{th} exceeds the end-to-end capacity C_{SD}, and is expressed as follows:

$$OP_{OMPB} = \Pr(C_{th} > C_{SD}) \tag{16}$$

$$OP_{OMPB} = \Pr(\min(SNR_{1v}, SNR_{2v}) < \theta) \tag{17}$$

$$OP_{OMPB} = \Pr(\max_{m=1,2,\ldots,M} (\min(SNR_{1v}, SNR_{2v})) < \theta) \tag{18}$$

where,

$$\theta = 2^{\frac{2C_{th}}{(1-\alpha)T}} - 1 \tag{19}$$

Then, the throughput (TP) can be formulated as in [23]:

$$TP_{OMPB} = (1-\alpha)TC_{th}(1 - OP_{OMPB}) \tag{20}$$

where (1 – α)T is the overall transmission time from the source passed by the relay to the destination.

4.2 OUTAGE PERFORMANCE FOR (H-PRS), (C-ORS), AND (B-ORS) ALGORITHMS, AND THROUGHPUT

As in [23], the general form of e2e OP for the three protocols is given as

$$OP_U = 1 - \Pr(\min(SNR_{1m}, SNR_{2m}) \geq \theta) \quad (21)$$

$$TP_U = (1-\alpha)TC_{th}(1-OP_U) \quad (22)$$

where,

$$U \in \{H-PRS, B-ORS, C-ORS\} \quad (23)$$

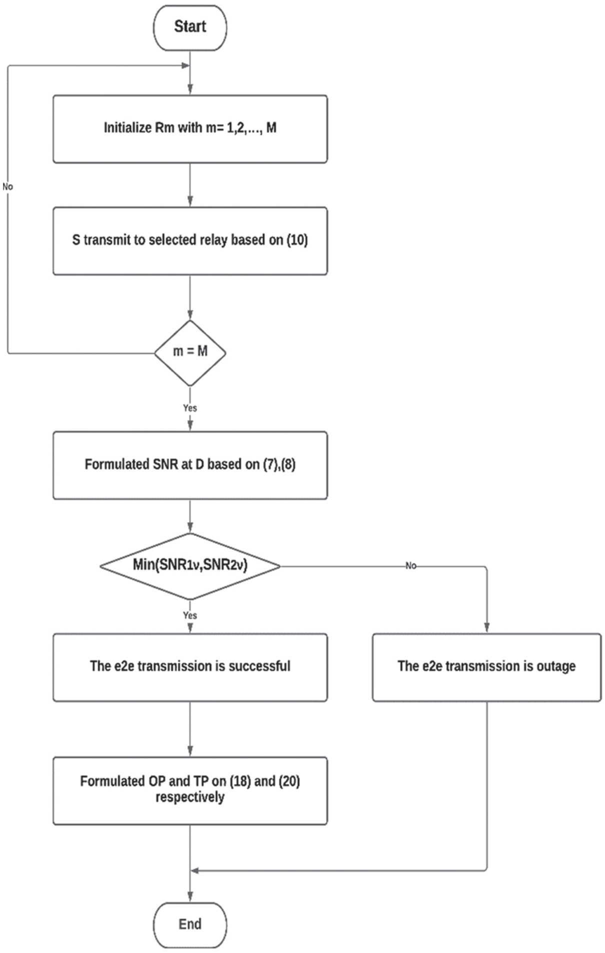

Fig. 3. The flow chart for the data transmission of OMPB-ORS scheme.

5. SIMULATION RESULTS

Here, the performance of the proposed protocol is presented. A set of numerical results is implemented under the existence of PUs provided with the interference constraints. To investigate the theoretical derivations, Monte-Carlo simulations are used. In TABLE 1, the WSN's nodes are organized in Cartesian coordinates in the simulation environment where S is located at the origin. The simulation, exact theoretical, and asymptotically theoretical results referred to them as (Sim), (Exact), and (Asym), respectively.

Table 1. System model parameters

System Parameters	Value
The number of relays	M = 2, 3, 4, and 5
The number of antennas of PB	K = 2
The transmission rate of S	C_{th} = 0.6, 0.7, and 1
Energy conversion efficiency	η = 1
Time block	T = 1
Harvesting time	α = 0.2s
Path-loss	β = 3
Ratio between Ith and PB	μ = 0.25
Number of PUs	N = 2
Relay coordinates	(X_R,0)
Destination coordinates	(1,0)
beacon coordinates	(0.5,0.5)
PU coordinates	(X_P, Y_P)

Fig. 4.compares the OP performance of the proposed protocol versus the H-PRS, C-ORS, and B-ORS protocols with C_{th} values. The proposed protocol has the lowest OP, and the H-PRS protocol has the highest. At a known high signal-to-noise ratio, the OP of the proposed, C-ORS and B-ORS protocols quickly decreased as Δ increased, which at Δ = 25 the enhancement percentages for the proposed protocol over H-PRS, C-ORS, and B-ORS protocols are 99.669%, 94.125%, and 94.20%, respectively, because the proposed, C-ORS and B-ORS protocols have a larger diversity gain than the H-PRS protocol.

To analyse the influence of distance on the proposed protocols' outage performance, OP was demonstrated as a function of the relay positions on the x-axis X_R. Fig. 5. Shows that the relays are in the best possible location, at which the proposed protocol OP value is lowest. Furthermore, when the relays are close to the destination, an intriguing consequence might be noticed, the OP values of the B-ORS and C-ORS protocols reach the OP of the proposed protocol. When the relays are extremely near the destination, the source-to-relay connection significantly impacts the OP of all protocols. Consequently, the B-ORS and C-ORS protocols are essentially equivalent to the proposed protocol.

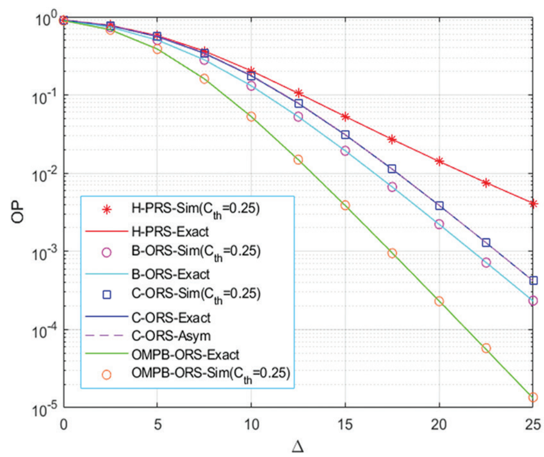

Fig. 4. OP as a function of Δ in dB when M = 2, X_R = 0.5, X_P = 0.5, Y_P = –0.5, α = 0.25, and $\tau_D^2 = \tau_1^2 = 0$

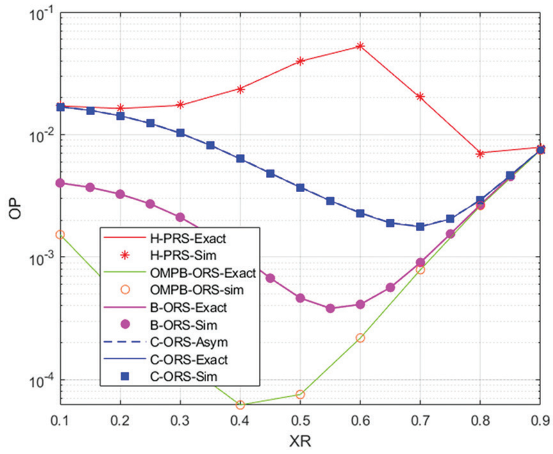

Fig. 5. OP as a function of X_R when $M = 4$, $X_P = 0.5$, $Y_P = -0.5$, $\alpha = 0.1$, $C_{th} = 0.6$, and $\tau_D^2 = 0.1$, and $\tau_1^2 = 0.05$.

Fig. 6. Explores the effect of the degree of hardware weakness τ_D^2 on the performance of all mentioned protocols. The OP values rapidly increase as τ_D^2 increases. Moreover, all protocols decrease when τ_D^2 exceeds 0.55.

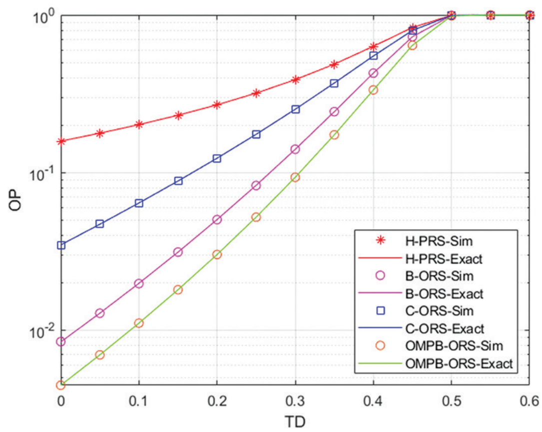

Fig. 6. OP as a function of τ_D^2 when $\Delta = 15$ dB, $M = 5$, $X_P = 0.5$, $Y_P = -0.5$, $\alpha = 0.1$, $C_{th} = 0.7$, and $\tau_1^2 = \tau_D^2/2$.

Fig. 7. Shows that TP is plotted as a function of the time spent on the EH process. As previously said, α value acts as a significant function in the EH operation because it affects the collected and transmitted power of the source or chosen relay node. There exist optimum values of where the proposed protocol TP is the best (Fig. 7.). Consider the following example: when the α-value is extremely low, PB can only gather a limited amount of energy. Consequently, the source or relay node can only transmit information with a minimal quantity of energy. When the α-value is too high, the data are relayed from the source to the destination with a lower effective transmission time, which decreases the overall TP. Consequently, the best TP performance may be attained for practical design when an optimum α-value is obtained. Fig. 7. shows that the enhancement percentages at α = 0.035 for the proposed protocol over the H-PRS, C-ORS, and B-ORS protocols are 23.7%, 18.1%, and 8.3467%, respectively. Finally, similar to the OP measure, the proposed TP performance is always the highest overall values. Fig. 7. shows that the enhancement percentages at α = 0.035 for the proposed protocol over H-PRS, C-ORS, and B-ORS protocols are 3%, 6.6%, and 10.2%, respectively.

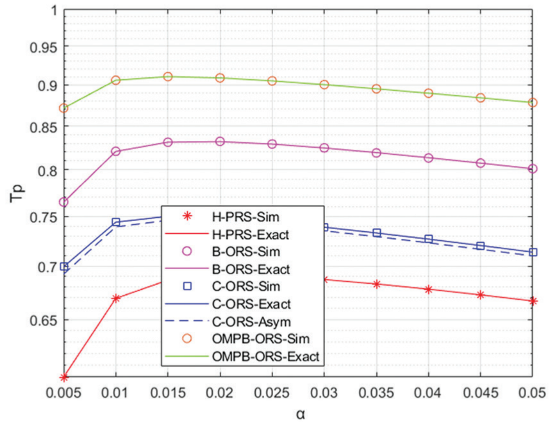

Fig. 7. TP as a function of α when $\Delta = 15$ dB, $M = 3$, $X_R = 0.5$, $X_P = 0.5$, $Y_P = -0.5$, $C_{th} = 1$, and $\tau_1^2 = \tau_D^2 = 0$

In Fig. 8., TP is shown against the number of relays. As predicted, increasing the M-value improves the TP of the OMPB-ORS, H-PRS, B-ORS, and C-ORS protocols. By effectively assigning the α-value, the performance of the investigated protocols can be enhanced.

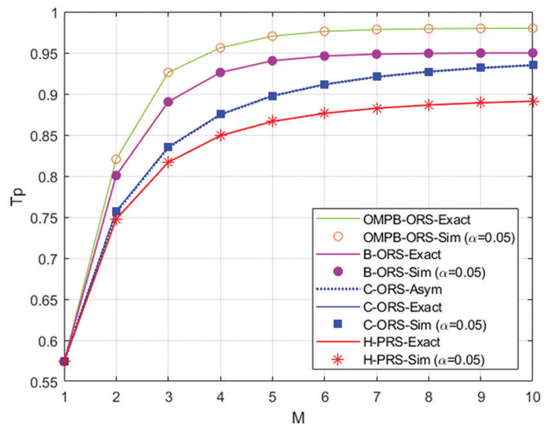

Fig. 8. TP as a function of M when $\Delta = 20$ dB, $M = 3$, $X_R = 0.4$, $X_P = 0.5$, $Y_P = -0.5$, $C_{th} = 1$, and $\tau_1^2 = 0.1$, $\tau_D^2 = 0.05$.

6. CONCLUSION

This study enhanced the performance of energy management systems based on WSN in intelligent structures under hardware weakness and interference restrictions. An OMPB-ORS protocol was proposed for EH relay networks using multiantenna PB, where PB supplies dual-hop DF relays and sources with RF signals to the EH process. In the presence of numerous PUs and across, i.e.,., Rayleigh-fading channels, exact and asymptotic formulations of the proposed protocol OP and TP were presented. The numerical results indicated that the OMPB-ORS protocol outperforms the B-ORS, C-ORS, and H-PRS protocols. Finally, by changing the energy harvesting ratio, increasing the number of relays, and locating the relays in the ideal place, the proposed protocol system's performance was improved.

7. REFERENCES

[1] R. L. Rosa, C. Dehollain, A. Burg, M. Costanza, P. Livreri, "An Energy-Autonomous Wireless Sensor with Simultaneous Energy Harvesting and Ambient Light Sensing", IEEE Sensors Journal, Vol. 21, No. 12, 2021, pp. 13744-13752.

[2] M. Li, C. Liu, Q. Li, "Energy Collaboration for Non-Homogeneous Energy Harvesting in Cooperative Wireless Sensor Networks", IEEE Access, Vol. 8, 2020, pp. 27027-27037.

[3] X. Liu, X. Yang, D. Ma, N. Jin, X. Lai, H. Tang, "A Novel Simultaneous Wireless Information and Power Transfer System", Proceedings of the IEEE Wireless Power Transfer Conference, 2019, pp. 212-215.

[4] C. Zhong, X. Chen, Z. Zhang, G. K. Karagiannidis, "Wireless-Powered Communications: Performance Analysis and Optimization", IEEE Transactions on Communications, Vol. 63, No. 12, 2015, pp. 5178-5190.

[5] C. Pan et al. "Intelligent Reflecting Surface Aided MIMO Broadcasting for Simultaneous Wireless Information and Power Transfer", IEEE Journal on Selected Areas in Communications, Vol. 38, No. 8, 2020, pp. 1719-1734.

[6] R. Zhang, C. K. Ho, "MIMO broadcasting for simultaneous wireless information and power transfer", IEEE Transactions on Wireless Communications, Vol. 12, No. 5, 2013, pp. 1989-2001.

[7] N. P. Le, "Throughput Analysis of Power-Beacon-Assisted Energy Harvesting Wireless Systems Over Non-Identical Nakagami-Fading Channels", IEEE Communications Letters, Vol. 22, No. 4, 2018, pp. 840-843.

[8] K. Huang, V. K. N. Lau, "Enabling Wireless Power Transfer in Cellular Networks: Architecture, Modeling and Deployment", IEEE Transactions on Wireless Communications, Vol. 13, No. 2, 2014, pp. 902-912.

[9] Y. Liu, L. Wang, S. A. Raza Zaidi, M. Elkashlan, T. Q. Duong, "Secure D2D Communication in Large-Scale Cognitive Cellular Networks: A Wireless Power Transfer Model", IEEE Transactions on Communications, Vol. 64, No. 1, 2016, pp. 329-342.

[10] M. N. Tehrani, M. Uysal, H. Yanikomeroglu, "Device-to-device communication in 5G cellular networks: challenges, solutions, and future directions", IEEE Communications Magazine, Vol. 52, No. 5, 2014, pp. 86-92.

[11] E. O. Kandaurova, D. S. Chirov, "Intelligent Algorithms for Dynamic Spectrum Access a Secondary User in Cognitive Radio Systems", Proceeding of the Systems of Signal Synchronization, Generating and Processing in Telecommunications, 2021, pp. 1-6.

[12] F. Kong, J. Cho, B. Lee, "Optimizing Spectrum Sensing Time with Adaptive Sensing Interval for Energy-Efficient CRSNs", IEEE Sensors Journal, Vol. 17, No. 22, 2017, pp. 7578-7588.

[13] L. T. Dung, T. D. Hieu, S. G. Choi, B. S. Kim, "An B. Impact of Beamforming on the Path Connectivity in Cognitive Radio Ad Hoc Networks", Sensors, Vol. 17, No. 4, 2017, p. 690.

[14] X. Deng, P. Guan, C. Hei, F. Li, J. Liu, N. Xiong, "An Intelligent Resource Allocation Scheme in Energy Harvesting Cognitive Wireless Sensor Networks", IEEE Transactions on Network Science and Engineering, Vol. 8, No. 2, 2021, pp. 1900-1912.

[15] M. Zheng, C. Wang, M. Song, W. Liang, H. Yu, "SACR: A Stability-Aware Cluster-Based Routing Protocol for Cognitive Radio Sensor Networks", IEEE Sensors Journal, Vol. 21, No. 15, 2021, pp. 17350-17359.

[16] A. A. Khan, M. H. Rehmani, A. Rachedi, "Cognitive-Radio-Based Internet of Things: Applications, Architectures, Spectrum Related Functionalities, and Future Research Directions", IEEE Wireless Communications, Vol. 24, No. 3, 2017, pp. 17-25.

[17] A. Bagheri, A. Ebrahimzadeh, "Statistical Analysis of Lifetime in Wireless Cognitive Sensor Network for Multi-Channel Cooperative Spectrum Sensing", IEEE Sensors Journal, Vol. 21, No. 2, pp. 2412-2421, 15 Jan.15, 2021.

[18] N. T. Tung, P. M. Nam, P. T. Tin, "Performance evalution of two-way with energy harvestin and hardware noises", Digital Communications and Networks, Vol. 7, No. 1, pp. 45-54, 2020.

[19] M. N. Pham, "On the secrecy outage probability and performance trade-off of the multi-hop cognitive relay networks", Telecommunication Systems, Vol. 73, 2020, pp. 349–358.

[20] S. Alvi, R. Hussain, Q. Hasan, S. Malik, "Improved buffer-aided multi-hop relaying with reduced outage and packet delay in cognitive radio networks", Electronics, Vol. 8, No. 8, 2019, p. 89.

[21] Shakeel A. Alvi, Riaz Hussain, Atif Shakeel, Muhammad Awais Javed, Qadeer Ul Hasan, Byung Moo Lee, Shahzad A. Malik, "QoS-Oriented Optimal Relay Selection in Cognitive Radio Networks", Wireless Communications and Mobile Computing, Vol. 2021, Article ID 5580963, 15 pages, 2021.

[22] D. H. Ha, T. N. Nguyen, M. H. Q. Tran, X. Li, P. T. Tran, M. Voznak, "Security and Reliability Analysis of a Two-Way Half-Duplex Wireless Relaying Network Using Partial Relay Selection and Hybrid TPSR Energy Harvesting at Relay Nodes", IEEE Access, Vol. 8, 2020, pp. 187165-187181.

[23] T. D. Hieu, T. T. Duy, L. T. Dung, S. G. Choi 2018. "Performance Evaluation of Relay Selection Schemes in Beacon-Assisted Dual-Hop Cognitive Radio Wireless Sensor Networks under Impact of Hardware Noises", Sensors, Vol. 18, No. 6, p. 1843.

[24] T. T. Duy, P. T. D. Ngoc, P. T. Tran, "Performance Enhancement for Multihop Cognitive DF and AF Relaying Protocols under Joint Impact of Interference and Hardware Noises: NOMA for Primary Network and Best-Path Selection for Secondary Network", Wireless Communications and Mobile Computing, Vol. 2021, Article ID 8861725, 15 pages, 2021.

[25] P. M. Quang, T. T. Duy, V. N. Q. Bao, "Performance Evaluation of Radio Frequency Energy Harvesting-Aided Multi-hop Cooperative Transmission Networks", Proceedings of the 25th Asia-Pacific Conference on Communications, 2019, pp. 521-526.

[26] H. V. Toan, Hoang, T. M. Duy, L. T. Dung, "Outage Probability and Ergodic Capacity of a Two-User NOMA Relaying System with an Energy Harvesting Full-Duplex Relay and Its Interference at the Near User", Sensors, Vol. 20, 2020, p. 6472.

[27] P. N. Son, T. T. Duy, K. Ho-Van, "SIC-Coding Schemes for Underlay Two-Way Relaying Cognitive Networks", Wireless Communications and Mobile Computing, Vol. 2020, Article ID 8860551, 17 pages, 2020.

[28] P. N. Son, T. T. Duy, "A new approach for two-way relaying networks: improving performance by successive interference cancellation, digital network coding and opportunistic relay selection", Wireless Networks, Vol. 26, 2020, pp. 1315–1329.

[29] T. N. Nguyen, T. H. Minh, P. T. Tran, M. Voznak, T. T. Duy, T. L. Nguyen, P. T. Tin, "Performance Enhancement for Energy Harvesting Based Two-way Relay Protocols in Wireless Ad-hoc Networks with Partial and Full Relay Selection Methods", Ad Hoc Networks, Vol. 84, 2019, pp. 178–187.

[30] D. T. Hoang, D. Niyato, P. Wang, D. I. Kim, "Opportunistic channel access and RF energy harvesting in cognitive radio networks", IEEE Journal on Selected Areas in Communication, Vol. 32, 2014, pp. 2039–2052.

[31] D. T. Hoang, D. Niyato, P. Wang, D. I. Kim, "Performance analysis of wireless energy harvesting cognitive radio networks under smart jamming attacks", IEEE Transactions on Cognitive Communication Networks, Vol. 1, 2015, pp. 200–216.

[32] D. K. Nguyen, D. Jayakody, S. Chatzinotas, J. S. Thompson, J. Li, "Wireless energy harvesting assisted two-way cognitive relay networks: Protocol design and performance analysis", IEEE Access, Vol. 5, 2017, pp. 21447–21460.

[33] C. Xu, M. Zheng, W. Liang, H. Yu, Y. C. Liang, "Outage performance of underlay multihop cognitive relay networks with energy harvesting", IEEE Communication Letters, Vol. 20, 2016, pp. 1148–1151.

[34] C. Xu, M. Zheng, W. Liang, H. Yu, Y. C. Liang, "End-to-end throughput maximization for underlay multihop cognitive radio networks with RF energy harvesting", IEEE Transactions on Wireless Communications, Vol. 16, 2017, pp. 3561–3572.

[35] E. Bjornson, M. Matthaiou, M. A. Debbah, "A new look at dual-hop relaying: Performance limits with hardware impairments", IEEE Transactions on Communication, Vol. 61, 2013, pp. 4512–4525.

[36] O. Messadi, A. Sali, V. Khodamoradi, A. Salah, G. Pan, S. J. Hashim, N. K. Noordin, "Optimal Relay Selection Scheme with Multiantenna Power Beacon

for Wireless-Powered Cooperation Communication Networks", Sensors, Vol. 21, 2021, p. 147.

[37] T. Yuan, M. Liu, Y. Feng, "Performance Analysis for SWIPT Cooperative DF Communication Systems with Hybrid Receiver and Non-Linear Energy Harvesting Model", Sensors, Vol. 20, 2020, p. 2472.

[38] H. Chen, Y. Li, J. L. Rebelatto, B. F. Uchoa-Filho,; B. Vucetic, "Harvest-then-cooperate: Wireless-powered cooperative communications", IEEE Transactions on Signal Processing, Vol. 63, 2015, pp. 1700–1711.

[39] T. N. Nguyen, M. Tran, D. H. Ha, T. T. Trang, M. Voznák, "Multi-source in DF Cooperative Networks with the PSR Protocol Based Full-Duplex Energy Harvesting over a Rayleigh Fading Channel: Performance Analysis", Proceedings of the Estonian Academy of Sciences, Vol. 68, 2019, pp. 264–275.

[40] P. T. Tin, B. H. Dinh, T. N. Nguyen, D. H. Ha, T. T. Trang, "Power Beacon-Assisted Energy Harvesting Wireless Physical Layer Cooperative Relaying Networks: Performance Analysis", Symmetry, Vol. 12, 2020, p. 106.

[41] T. M. Hoang, N. T. Tan, X. N. Tran, "Performance analysis of power beacon-assisted energy harvesting NOMA multi-user relaying system over Nakagami-m fading channels", International Journal of Electronics and Communications, Vol. 115, 2020, p. 153022.

[42] P. K. Sharma, P. K. Upadhyay, "Cognitive relaying with transceiver hardware impairments under interference constraints", IEEE Communication Letters, Vol. 20, 2016, pp. 820–823.

[43] N. T. Do, V. Bao, B. An, "Outage performance analysis of relay selection schemes in wireless energy harvesting cooperative networks over non-identical rayleigh fading channels", Sensors, Vol. 16, 2016, p. 295.